Title
SPATIALLY SELECTIVE NMR WITH BROADBAND RADIOFREQUENCY PULSES

Authors
Baum, J.
Tycko, R.
Pines, A.

Publication Date
1985-12-01

LBL-20921
Preprint c.2

Lawrence Berkeley Laboratory
UNIVERSITY OF CALIFORNIA

Materials & Molecular Research Division

Submitted to Chemical Physics

SPATIALLY SELECTIVE NMR WITH
BROADBAND RADIOFREQUENCY PULSES

J. Baum, R. Tycko, and A. Pines

December 1985

Prepared for the U.S. Department of Energy under Contract DE-AC03-76SF00098

DISCLAIMER

SPATIALLY SELECTIVE NMR WITH BROADBAND RADIOFREQUENCY PULSES

J. Baum, R. Tycko[a], and A. Pines*

Department of Chemistry, University of California, Berkeley and

Materials and Molecular Research Division, Lawrence Berkeley Laboratory,

Berkeley, CA 94720

[a]Current address: Department of Chemistry, University of Pennsylvania, Philadelphia, PA 19104.

This work was supported by the Director, Office of Energy Research, Office of Basic Energy Sciences, Materials Sciences Division of the U.S. Department of Energy and by the Director's Program Devlopment Funds of the Lawrence Berkeley Laboratory under Contract No. DE-AC03-76SF00098.

Abstract

The problem of non-invasive spatial localization in NMR is approached by constructing a spatially selective composite pulse sequence and incorporating it into a recently developed difference scheme. The composite sequence described, which requires 9 phase shifted π pulses, functions only over a narrow range of radio-frequency (RF) field strengths while remaining effective over a broad range of resonance frequencies. Relying upon the field gradient of a surface coil to label regions in space by local RF amplitudes, the pulse inverts all nuclear spins at a selected distance from the coil across a broad range of chemical shifts. This approach will allow the observation of chemically shifted NMR signals from specific regions of a material or organism. Computer simulations are presented, and the method is demonstrated experimentally on a phantom sample using a surface coil.

1. Introduction

It is often useful in many areas of chemistry to be able to obtain spectroscopic information from a localized region of a sample noninvasively. Spatial localization is desirable in a number of systems, ranging from heterogeneous solids such as coals, catalysts and semiconductors to living tissues and organisms. For example, the elucidation of the action of a catalyst may be aided considerably by restricting observed signals to those originating from the surface layer alone, eliminating the otherwise overwhelming contribution from the bulk. The need for spatial localization is also felt keenly in *in vivo* NMR and magnetic resonance imaging, where signal frequently must be obtained from a selected organ without interference from surrounding tissues. Thus spatially selective excitation, which can be directed at specific sites in a heterogeneous system and which can yield accurate chemical information from these sites, is a highly desirable goal for spectroscopy in general and NMR in particular.

In a recent Communication[1], we introduced a technique designed to localize NMR signals in space by combining the radio-frequency (rf) gradient of a surface coil[2] with an excitation sequence narrowband in rf field strength.[3-6] The excitation sequence is a variant of a composite π pulse[7] that inverts spin populations only within a small range of rf field amplitudes. This paper enlarges upon the earlier work in three important areas. First, a pulse sequence is suggested that has the required narrowband properties with respect to the rf amplitude but at the same time uniformly exictes over a substantial range of resonant frequencies. This allows the technique to be used in situations where the observed signals span a large chemical shift range, without requiring unreasonably high rf power. Second, experimental results on a phantom sample and using a surface coil are given to demonstrate both the degree of spatial localization that may be achieved and the chemical shift range that may be covered. Third, we present a brief discussion of the relationship of our method to spatial localization methods proposed by other authors, with the intent of pointing out the experimental conditions under which different techniques may be preferred.

2. Development of Pulse Sequences

a. **Narrowband Localized Excitation (NOBLE).** A NOBLE pulse sequence is comprised of two parts.[1] The first is a narrowband inversion sequence P, which inverts spin populations in a narrow range of rf amplitudes centered about a nominal value ω_1^0(rad/sec). The second is a read sequence R, which in the simplest case may be single pulse. The free induction decay (FID) after applying P and R in succession is subtracted from the FID after R alone. The remaining signal arises only from those regions in space where P inverts spins and R excites signal. Signal contributions due to residual transverse magnetization created by P are eliminated either by dephasing in a delay between P and R or by phase cycling of P. Dephasing may result from an applied pulsed static field gradient, or from transverse relaxation if $T_2 < T_1$.

This method leads to very simple expressions for the signal amplitude and phase. Suppose that P produces an inversion $W(\omega_1, \Delta\omega)$ at an rf amplitude ω_1 and a resonance offset $\Delta\omega$, where W is defined as usual [1,3-7] to run between -1 and 1, with -1 indicating equilibrium spin populations and 1 indicating complete population inversion. In addition, suppose that R excites transverse magnetization with an amplitude $A(\omega_1,\Delta\omega)$ and a phase $\phi(\omega_1,\Delta\omega)$. Then the signal amplitude is proportional to $S(\omega_1,\Delta\omega)$, given by

$$S(\omega_1,\Delta\omega) = [1 + W(\omega_1,\Delta\omega)]\, A(\omega_1,\Delta\omega) \qquad [1]$$

and the signal phase is $\phi(\omega_1,\Delta\omega)$. An additional factor of ω_1 would be present in Eq. [1], arising from the detection efficiency, if the same surface coil were used for both excitation and detection.[8] The fact that the signal phase depends only on R is significant. In general, the direction of the net rotation axis of P, loosely speaking the "phase" of P, changes considerably with ω_1. If the signal phase were to depend on the phase of P, contributions to the total acquired signal with different values of ω_1 and the same value of $\Delta\omega$ could interfere destructively.[9] Thus, a loss of sensitivity would result. NOBLE avoids this problem, since only the inversion produced by P and not the phase plays a role.

b. **Selective inversion sequences.** There remains considerable flexibility in the choice of specific sequences for P and R, subject to the constraint that the duration of the sequences must be short compared to T_1 and T_2. Narrowband sequences have been derived using iterative schemes by our laboratory[3,4] and by Shaka and Freeman.[5] The iterative schemes can generate pulse sequences with arbitrarily small bandwidths in ω_1. Typically, however, the bandwidths in $\Delta\omega$ are also small, i.e. $W(\omega_1,\Delta\omega)$ is a strong function of $\Delta\omega$ as well as ω_1. Using fixed point methods, some progress has been made towards the development of iterative schemes for generating inversion sequences that are narrowband with respect to ω_1 and broadband with respect to $\Delta\omega$.[4] For the present purpose, however, we programmed a computer to search for sequences that meet given bandwidth criteria. It was found that less than nine pulses do not meet the inversion profile requirements over both of ω_1 and $\Delta\omega$. Therefore, in a typical search, the program examines all pulse sequences composed of nine pulses with nominal flip angles of 180° and with the individual phases in multiples of 15°. The desired values of $W(\omega_1,\Delta\omega)$ are specified for 26 combinations of ω_1 and $\Delta\omega$. The actual values of $W(\omega_1,\Delta\omega)$ are calculated for each possible sequence. The sequence with the smallest variance between the actual $W(\omega_1,\Delta\omega)$ values and the desired $W(\omega_1,\Delta\omega)$ values is selected. Only sequences with symmetric phases are considered, reducing the number of sequences that must be tested and eliminating the need to examine both positive and negative values of $\Delta\omega$[10] Once a sequence is found, it can be refined by changing the pulse phases in 5° increment. Simulations indicate that phase errors within 5° of the nominal phase do not appreciably alter the inversion profiles, therefore further refinement of the pulse phases is not necessary.

The sequence $180_{30}180_{205}180_{230}180_{85}180_{0}180_{85}180_{230}180_{205}180_{30}$, which we denote P_0, results from such a search procedure. The contour plot in Figure 1 illustrates the inversion performance. According to Eq. [1], P_0 allows the signal amplitude at $\omega_1 = \omega_1^0$ to be greater than 75% of its maximum for all resonance offsets in the range $-0.3\omega_1^0 < \Delta\omega < 0.3\omega_1^0$. Significant signal at undesired values of ω_1 can only develop when $|\Delta\omega| > 0.3\omega_1^0$.

c. **Read sequences.** Any sequence composed of an odd number of nominal 180° pulses such as P_0, will invert spin populations when ω_1 is any odd multiple of ω_1^0. Thus large signal contributions may arise from regions in space where ω_1 is approximately an odd multiple of ω_1^0 in addition to the desired region where ω_1 is approximately equal to ω_1^0. In reference 1, we suggested using a single nominal 60° pulse for R. A nominal 60° pulse becomes a 180° pulse at $\omega_1 = 3\omega_1^0$, making $A(3\omega_1^0,0) = 0$. Bendall has demonstrated the same approach for suppressing high flux signals with depth pulses.[11,12] In Figure 2a, we show a plot of $S(\omega_1,0)$ for NOBLE using P_0 and a nominal 60° pulse for R. Although $S(3\omega_1^0,0) = 0$, there is substantial signal on either side of $3\omega_1^0$. Signals on opposite sides of $3\omega_1^0$ have opposite phases so that partial cancellation may be expected, but the suppression is not ideal. The signal at ω_1^0 is reduced from its maximum factor of 3/2, since it is excited by a 60° pulse rather than a 90° pulse. In addition, as can be seen in Figure 2b, a 60° pulse is not broadband over the desired range of frenquency offsets.

A better choice for R would have the following three properties. First, it would be a broadband inversion sequence near $3\omega_1^0$, inverting spins and exciting no signal over large ranges of both ω_1 and $\Delta\omega$. Second, it would excite nearly the maximum signal at $\omega_1 = \omega_1^0$. A sequence that has these properties is $90_{180}120_0 30_{90}90_{270}120_{90}30_0$, which we denote R_0. R_0 is derived from the composite π pulse $270_{180}360_0 90_{90}270_{270}360_{90}90_0$ developed by Shaka and Freeman,[13] simply by dividing all pulse lengths by three. That R_0 has the first property above is a consequence of the work of Shaka and Freeman;[13] that it has the other two properties might be coincidental. Figures 2c, and 2d are plots of $S(\omega_1,\Delta\omega)$ for NOBLE using P_0 and R_0. The selectivity with respect to ω_1 and the useful range of $\Delta\omega$ are illustrated; the signal profile is essentially identical between $\Delta\omega = 0$ and $\Delta\omega = 0.2$.

At this point, we stress that other choices for P and R are possible. P_0 and R_0 were selected principally to provide a large bandwidth in $\Delta\omega$ and to eliminate signal contributions from the $3\omega_1^0$ region. Other considerations may require different sequences, for example a P with a narrower bandwidth in ω_1 in order to produce finer spatial resolution.[1,3-5] Read sequences that do not excite signal at higher multiples of ω_1, e.g. both $3\omega_1^0$ and $5\omega_1^0$, can be found.

A potentially important possibility is the use of an adiabatic frequency sweep[14] or an equivalent phase modulated pulse[15-17] as the read sequence. Adiabatic sweeps can invert spins essentially completely for arbitrarily large values of ω_1 above a threshold ω_1^t that depends on the sweep rate.[16,17] Below ω_1^t, the conditions for adiabaticity[17] are not satisfied and transverse magnetization is created. Thus by placing the threshold between ω_1^0 and $3\omega_1^0$, all contributions to the signal except those near ω_1^0 could be eliminated. In addition, if the fine spatial resolution afforded by P is not required, an adiabatic sweep could be used alone. This would be an entirely new approach to spatial localization.

3. Experimental Demonstration of NOBLE

a. **Experimental design.** Experiments were performed at 180 MHz on a phantom sample of $H_2O(\ell)$ using a three turn surface coil. The configuration of the sample and coil is shown in Fig. 3a. The sample consists of a 10 mm long section of delrin rod with a diameter of 4 mm, into which five holes have been drilled with a spacing of 2.0 mm. The holes are filled with $H_2O(\ell)$ and are labelled as positions 1 through 5 in order of increasing distance from the plane of the coil. The coil diameter is 1.5 cm. To provide a one-dimensional image of the sample, a pulsed field gradient of approximately 1.14 Gcm^{-1} is applied along the long axis of the sample. Fig. 3b is a one-dimensional image of the phantom sample obtained by giving a single pulse and Fourier transforming the ensuing FID. Signals from positions 1 through 5 are clearly distinguished. The decrease in signal intensity with increasing number is a consequence of both the smaller pulse flip angle and the reduced detection efficiency with increasing distance from the surface coil. The value of $\omega_1/2\pi$ at each position was determined by adjusting the pulse length so as to produce a null of the signal. In order of increasing position number, the values are 33, 21, 12.5, 7.9 and 4.9 kHz. The experimental timing sequence is shown is Fig. 4. The static field gradient serves only to allow a direct visualization of the spatial distribution of signal contributions for demonstration purposes and, less importantly, to cause transverse magnetization to dephase during τ in Fig. 4. The static field gradient is not a relevant component of the spatial selectivity of NOBLE.

b. **Experimental results.** Fig. 5 illustrates the degree of spatial localization resulting from NOBLE. Fig. 5a is the image resulting from excitation by R_0; Fig. 5b is the image resulting from excitation by R_0 after inversion by P_0. The pulse lengths are adjsuted according to the rf amplitude at position 3, i.e. ω_1^0 = 12.5 kHz. Fig. 5c is the difference of Figs. 5a and 5b. Appreciable signal remains at position 3 only.

The resonance offset range of the P_0 and R_0 sequences is demonstrated in Figure 6. NOBLE is applied with the pulse lengths adjusted to localize the signal to position 3. Without changing the pulse lengths, the rf carrier frequency is changed in increments of 1000 Hz. Good localization is preserved up to resonance offsets of 3000 Hz, or $\omega/\omega^0{}_1$ = 0.24.

4. Discussion of Spatial Localization Methods

Various methods for spatially localizing NMR signals, with the preservation of spectral information, have been developed. Some of these rely on static field gradients,[18-29] some rely on rf field gradients,[1,5-6,11-12,30-39] and some rely on a combination of the two.[11,40] Methods that rely on static field gradients have the advantage that signals can in principle be localized to a well-restricted sensitive volume, for example a cube. They have the disadvantage that pulsed gradients in three independent directions are required for localization in three dimensions. Methods that rely on rf field gradients have the advantage of comparative simplicity, insofar as probe or magnet design is concerned, and can exploit the sensitivity advantage and partial localization inherent in surface coils.[2,41] The major disadvantage of rf gradient methods, including NOBLE, is the diffuse sensitive volume, as determined by the shapes of surfaces of constant transverse rf fields. Spatial localization achieved by the selection of a particular value of the of the B_1 field is not necessarily restricted to a point on the axis of the surface coil but will also occur along the transverse component of the rf field. This results in a sensitive volume whose shape is defined by the rf field profile of the surface coil. This disadvantage can be overcome to an extent by alternative coil geometries,[42] multiple excitation coils,[36] separate excitation and detection coils,[34] and the combination of rf and static field gradients.[11,40]

For the present discussion, we limit ourselves to rf gradient methods. In addition to NOBLE, there are two other techniques that have been developed to date to acquire NMR signals only from a limited spatial region in an rf gradient. One of these, that of Shaka et al.,[5,6] also makes use of narrowband inversion sequences. Signals from outside the region of interest are eliminated in a phase cycling scheme involving the coaddition of four[5] or sixteen[6] FID signals. Provided that the same inversion sequence is used, the sensitive volumes of NOBLE and the four step version of Shaka et al. are the same. The latter method is susceptible to destructive interference within the sensitive volume arising from phase variations in the inversion sequence as discussed above. Whether this proves to be a significant distinction in practice is determined by the choice of the inversion sequence and by the signal distribution within the sensitive volume. The sequence $180_0 180_{270} 180_{180}$ demonstrated by Shaka et al.[6] produces no phase variations on resonance, a consequence of the antisymmetric rf phases of such sequences. Shaka and Freeman have also described another method designed to function over a large range of resonance offsets.[39] Here, composite prepulses, broadband in both $\Delta\omega$ and ω_1, are incorporated into phase cycling schemes in order to achieve the desired localization. As more prepulses are applied, the ω_1 profile becomes progressively narrower. The best signal profile, which covers a large range of resonance offsets and is narrowband in rf field strength, arises from a 24 stage scheme containing three prepulses. The phase of the signal is well behaved with this method.

The second technique is the depth pulse method of Bendall et al.[11-12,33-38] Depth pulse sequences all consist of strings of pulses combined with specific phase cycling schemes. The pulses themselves do not possess narrowband properties. Rather, the sensitivity to the rf amplitude results from the extensive phase cycling, which cancels signals from undesired spatial regions. Thus, the depth pulse method is conceptually quite different from NOBLE, arising out of the phase cycling tradition in NMR rather than the more recent composite pulse tradition.[7]

Depth pulse sequences that provide localization in the vicinity of $\omega_1 = \omega_1^0$ similar to that in Fig. 2 require the coaddition of 16 or more FID signals.[12] Procedures for eliminating signal from the $3\omega_1^0$ and $5\omega_1^0$ regions have been suggested, and require 32 and 64 FIDS respectively.[11] The useful resonance offset ranges of the depth pulse sequences are similar to that exhibited using P_0 and R_0.

We expect NOBLE, when combined with a suitable inversion pulse, to be useful under a number of relevant experimental conditions. First consider a situation in which the intrinsic signal to noise ratio is high and in which time is limited. In this case, NOBLE offers the advantage of good time resolution. In addition to the requirement of fewer FID signals, NOBLE can be repeated with an arbitrarily short recycle delay without appreciable degradation of the spatial selectivity. This is because the longitudinal magnetization before each shot in the undesired spatial regions is a constant, independent of the pulse phases in the previous shot, once a steady state is reached. Rapid pulsing can lead to a greater signal to noise ratio in a fixed time.

Another important limit is an experiment with a low intrinsic signal to noise ratio and with no time constraint. In such an experiment, none of the techniques has an overriding, intrinsic advantage. A decision is likely to be made on the basis of experimental convenience. The use of separate excitation and detection coils,[34] and the use of multiple excitation coils to restrict the sensitive volume have been developed for depth pulses by Bendall et al.[36] Ideally, these ingenious multiple coil experiments could be combined with the selectivity of NOBLE.

An alternative for experiments in which considerable signal averaging is permitted or required is to use a rotating frame chemical shift imaging (RFCSI) technique.[30-32] Briefly, a two-dimensional RFCSI experiment consists of collecting a series of FIDS, acquired in the intervals labelled by t_2, following excitation by a pulse of variable length t_1, from a surface coil or other source of an inhomogeneous rf field. A double Fourier transform yields a two-dimensional "spectrum" with spectral information along one axis and rf strength, i.e. distance, information along the other axis. RFCSI clearly differs from NOBLE and depth pulse sequences in that signal from all spatial regions is preserved but is separated by the Fourier transformation with respect to t_1. In order to achieve a spatial resolution and extent comparable to that in Figures 2 and 5, a minimum of approximately 16 values of t_1 would have to be sampled. Thus the minimum time for an RFCSI experiment is comparable to that of a depth pulse experiment, but is eight times greater than that of a NOBLE experiment. The signal to noise ratio in an RFCSI spectrum is expected to be less than that in a depth pulse or NOBLE spectrum by a factor on the order of 2 for a fixed total number of acquired FIDS.[30] However, spectral information from all spatial regions is acquired at once, making for greater efficiency if such information is desired. In a sense, the relationship of RFCSI to depth pulses and NOBLE is analogous to the relationship of sensitive line methods to sensitive point methods, as explained in discussions of NMR imaging.[43-45]

5. Conclusion

We have presented a composite pulse sequence, narrowband in space and broadband in frequency, which can be used in conjunction with a surface coil to acquire a chemically shifted NMR signal from a localized region of a sample. The 9 pulse population inversion sequence, used in the NOBLE method, spatially localizes signals in an rf field gradient to a region where the rf amplitude ω_1 approximately satisfies $0.75\omega_1^0 < \omega_1 < 1.25\omega_1^0$, and retains a useful resonance offset range of $-0.3\omega_1^0 < \Delta\omega < 0.3\omega_1^0$. Undesired signals arising from spatial regions where ω_1 is approximately $3\omega_1^0$ are suppressed by using a read sequence that is a broadband composite π pulse near $3\omega_1^0$. It is suggested that adiabatic frequency sweeps may be used to suppress signals from regions where ω_1 is a higher multiple of ω_1^0. A combination of these selective techniques with SHARP spectroscopy[46] may allow high resolution surface coil NMR in the presence of inhomogeneous static fields.

Acknowledgment

This work was supported by the Director, Office of Energy Research, Office of Basic Energy Services, Materials Sciences Division of the U.S. Department of Energy and by the Director's Program Development Funds of the Lawrence Berkeley Laboratory under Contract No. DE-AC03-76F00098.

References

1. R. Tycko and A. Pines, J. Magn. Reson. **60**, 156-160 (1984).

2. J.J.H. Ackerman, T.H. Grove, G.C. Wong, and G.K. Radda, Nature (London) **283**, 167-170 (1980).

3. R. Tycko and A. Pines, Chem. Phys. Lett., **111**, 462-467 (1984).

4. R. Tycko, J. Guckenheimer, and A. Pines, J. Chem, Phys., **83**, 2775-2802 (1985) .

5. A.J. Shaka and R. Freeman, J. Magn. Reson. **59**, 169-176 (1984).

6. A.J. Shaka, J. Keeler, M.B. Smith, and R. Freeman, J. Magn. Reson. **61**, 175-180 (1985).

7. M.H. Levitt and R. Freeman, J. Magn. Reson. **33**, 473-476 (1979).

8. D.I. Hoult and R.E. Richards, J. Magn. Reson. **24**, 71 (1976).

9. R. Tycko, H.M. Cho, E. Schneider, and A. Pines, J. Magn. Reson. **61**, 90-101 (1985).

10. M.H. Levitt, J. Magn. Reson. **48**, 234-264 (1982).

11. M.R. Bendall, J. Magn. Reson. **59**, 406-429 (1984).

12. M.R. Bendall, in Biomedical Magnetic Resonance. (T.L. James and A.R. Margulis, eds.) p.99, Radiology Research and Education Foundation, San Francisco, 1984.

13. A.J. Shaka and R. Freeman, J. Magn. Reson. **55**, 487-493 (1983).

14. A. Abragam, Principles of Nuclear Magnetism (Oxford University Press, Oxford, 1961), p.44.

15. L. Allen and J.H. Eberley, Optical Resonance and Two Level Atoms (Wiley, New York, 1975), p. 101.

16. J. Baum, R. Tycko, and A. Pines, J. Chem. Phys. **79**, 4643-4644 (1983).

17. J. Baum, R. Tycko, and A. Pines, Phys. Rev. A. **32**, 3435 (1985)

18. P. Bendel, C.M. Lai, and P.C. Lauterbur, J. Magn. Reson. **38**,343-356 (1980).

19. P.C. Lauterbur, D.N. Levin, and R.B. Marr, J. Magn. Reson. **59**, 536-541 (1984).

20. M.L. Bernardo Jr., P.C. Lauterbur, and L.K. Hedges, J. Magn. Reson. **61**,

168 (1985).

21. A. Kumar, D. Welti, and R.R. Ernst, J. Magn. Reson. 18, 69-83 (1975).

22. T.R. Brown, B.M. Kincaid, and K. Ugurbil, Proc. Nat. Acad. Sci. USA 79, 3523 (1982).

23. A.A. Maudsley, S.K. Hilal, W.H. Perman, and H.E. Simon, J. Magn. Reson. **51**, 147-152 (1983).

24. J.F. Martin and C.G. Wade, J. Magn. Reson. **61**, 153 (1985).

25. P.C. Lauterbur, D.M. Kramer, W.V. House Jr., and C.N. Chen, J. Am. Chem. Soc. **97**, 6866 (1975).

26. W.P. Aue, S. Müller, T.A. Cross, and J. Seelig, J. Magn. Reson. **56**, 350-354 (1984).

27. R.E. Gordon, P.E. Hanley, D. Shaw, D.G. Gadian, G.K. Radda, P. Styles, P.J. Bore, and L. Chan, Nature (London) **287**, 736-738 (1980).

28. P.A. Bottomley, J. Magn. Reson. **50**, 335 (1982).

29. K.N. Scott, H.R. Brooker, J.R. Fitzsimmons, H.F. Bennet, and R.C. Mick, J. Magn. Reson. **50**, 339-344 (1982).

30. D.I. Hoult, J. Magn. Reson. **33**, 183-197 (1979).

31. S. Cox and P. Styles, J. Magn. Reson. **40**, 209 (1980).

32. A. Haase, C. Malloy, and G.K. Radda, J. Magn. Reson. **55**, 164-169 (1983).

33. M.R. Bendall and R.E. Gordon, J. Magn. Reson. **53**, 365-385 (1983).

34. M.R. Bendall, Chem. Phys. Lett. **99**, 310-315 (1983).

35. M.R. Bendall and W.P. Aue, J. Magn. Reson. **54**, 149-152 (1983).

36. M.R. Bendall, J.M. McKendry, I.D. Cresshull, and R.J. Ordidge, J. Magn. Reson. **60**, 473-478 (1984).

37. M.R. Bendall, Magn. Reson. in Med. **2**, 91 (1985).

38. M.R. Bendall and D.T. Pegg, J. Magn. Reson. **63**, 494-503 (1985).

39. A.J. Shaka and R. Freeman, J. Magn. Reson. **64**, 145-150 (1985).

40. P.A. Bottomley, T.B. Foster, and R.D. Darrow, J. Magn. Reson. **59**, 338-342 (1984).

41. J.L. Evelhoch, M.G. Crowley, and J.J.H. Ackerman, J. Magn. Reson. **56**,

110-124 (1984).

42. M.S. Roos, A. Hasenfeld, M.R. Bendall, R.H. Huesman, and T.F. Budinger, presented at the Third Annual Meeting of the Society of Magnetic Resonance in Medicine, New York, 1984.

43. P. Brunner and R.R. Ernst, J. Magn. Reson. 33, 83-106 (1979).

44. P.A. Bottomley, Rev. Sci. Instrum. 53, 1319 (1982).

45. P. Mansfield and P.G. Morris, "NMR Imaging in Biomedicine" (Academic Press, New York, 1982).

46. M. Gochin and A. Pines, J. Am. Chem. Soc., in press. Gochin, M.; Weitekamp, D.P.; Pines, A. J. Magn. Reson. 63, 431-437 (1985)

Figure 1

Contour plot of inversion performance versus resonance offset ($\Delta\omega/\omega_1^0$) and rf field strength (ω_1/ω_1^0) for the composite pulse sequence P_0: $180_{30}180_{205}180_{230}180_{85}180_{0}180_{85}180_{230}180_{205}180_{30}$. Each pulse is specified by two angles, θ_ϕ, where θ denotes the flip angle and ϕ the phase. P_0 produces narrowband inversion with respect to ω_1 and broadband inversion with respect to $\Delta\omega$.

Figure 2

Simulations of NOBLE signal amplitude $S(\omega_1,\Delta\omega)$ with the inversion pulse P_0, as specified in Fig. 1, and various read sequences R:

a) $S(\omega_1, 0)$ for $R = \pi/3$

b) $S(\omega_1, 0.2\omega_1^0)$ for $R = \pi/3$

c) $S(\omega_1, 0)$ for $R_0 = 90_{180}120_{0}30_{90}90_{270}120_{90}30_{0}$

d) $S(\omega_1, 0.2\omega_1^0)$ for $R_0 = 90_{180}120_{0}30_{90}90_{270}120_{90}30_{0}$

An additional factor of ω_1 arising from the detection efficiency with a surface coil is included. The read sequence R_0 of (c) and (d) effectively eliminates the signals from the $3\omega_1^0$ region while maintaining almost maximum intensity in the ω_1^0 region.

Figure 3

Top: Surface coil and sample geometry

The sample consists of a delrin rod (4mm diameter) containing 5 small holes filled with $H_2O(\ell)$.

Bottom: ^1H spectrum of the phantom sample recorded after a $\pi/2$ pulse at position 1. A static field gradient is used to obtain the one dimensional image.

Figure 4: Experimental timing diagram.

The selective inversion pulse, P_0, shown in Fig. 1 is followed by a period τ, during which transverse magnetization is allowed to dephase. The free induction decay is recorded following the read pulse, R_0, of Fig. 2c. A pulsed static field gradient along the long axis is used to provide the one dimensional image of the phantom containing $H_2O(\ell)$. The NOBLE experiment is performed by subtracting the inverted signal from the FID obtained after R_0 alone. The signal that results when the pulses are applied with a surface coil arises only from a localized region in space.

Figure 5:

^1H spectra obtained according to the NOBLE method for the phantom water sample shown. Pulse lengths were calibrated with reference to the nominal rf amplitude, $\omega_1^0 = 12.5$ kHz, existing at position 3.

a) $R_0 = 90_{180}120_0 30_{90}90_{270}120_{90}30_0$. The spectrum contains signals from all five bulbs.

b) Spectrum read by R_0 following a spatially selective inversion pulse, $P_0 = 180_{30}180_{205}180_{230}180_{85}180_0 180_{85}180_{230}180_{205}180_{30}$, adjusted for bulb 3.

c) Difference spectrum obtained by subtracting b) from a). Only signal from position 3 is retained in this spatially localized spectrum.

Figure 6

Stacked plot illustrating the broadband properties of the composite inversion pulse with respect to resonance offset. Each peak is a spatially localized signal from bulb 3, obtained under NOBLE with frequency offset as marked. Spatial selectivity is achieved successfully up to a frequency offset of approximately 25% of the nominal rf amplitude.

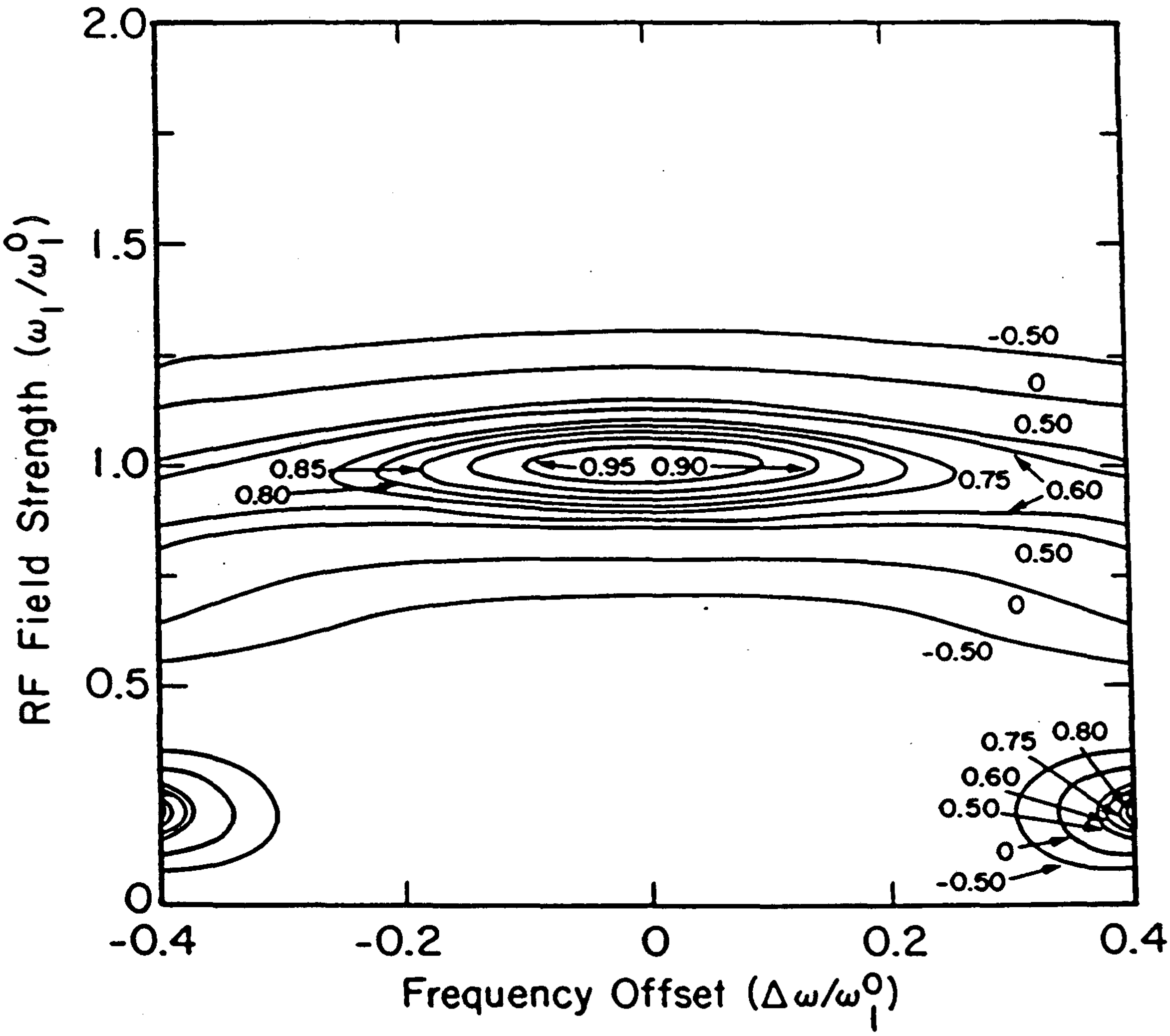
2.0
1.5
1.0
0.5
0
RF Field Strength (ω_1/ω_1^0)
-0.4
-0.2
0
0.2
0.4
Frequency Offset $(\Delta\omega/\omega_1^0)$
-0.50
0
0.50
0.85
0.80
0.95
0.90
0.75
0.60
0.50
0
-0.50
0.75
0.80
0.60
0.50
0
-0.50

Figure 1

Figure 2

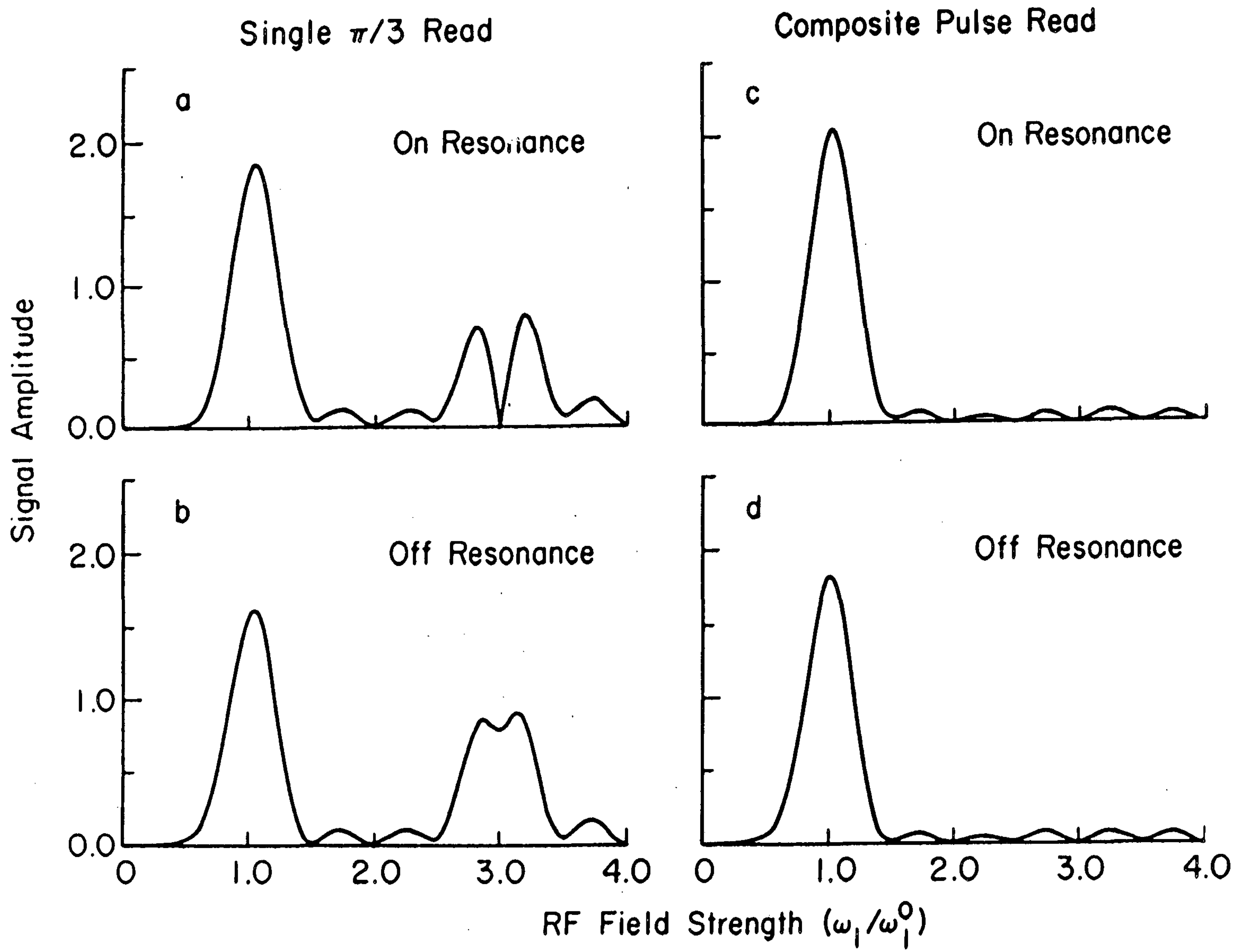

Single π/3 Read
Composite Pulse Read
a
On Resonance
b
Off Resonance
c
On Resonance
d
Off Resonance
Signal Amplitude
0.0
1.0
2.0
0
1.0
2.0
3.0
4.0
RF Field Strength (ω_1/ω_1^0)

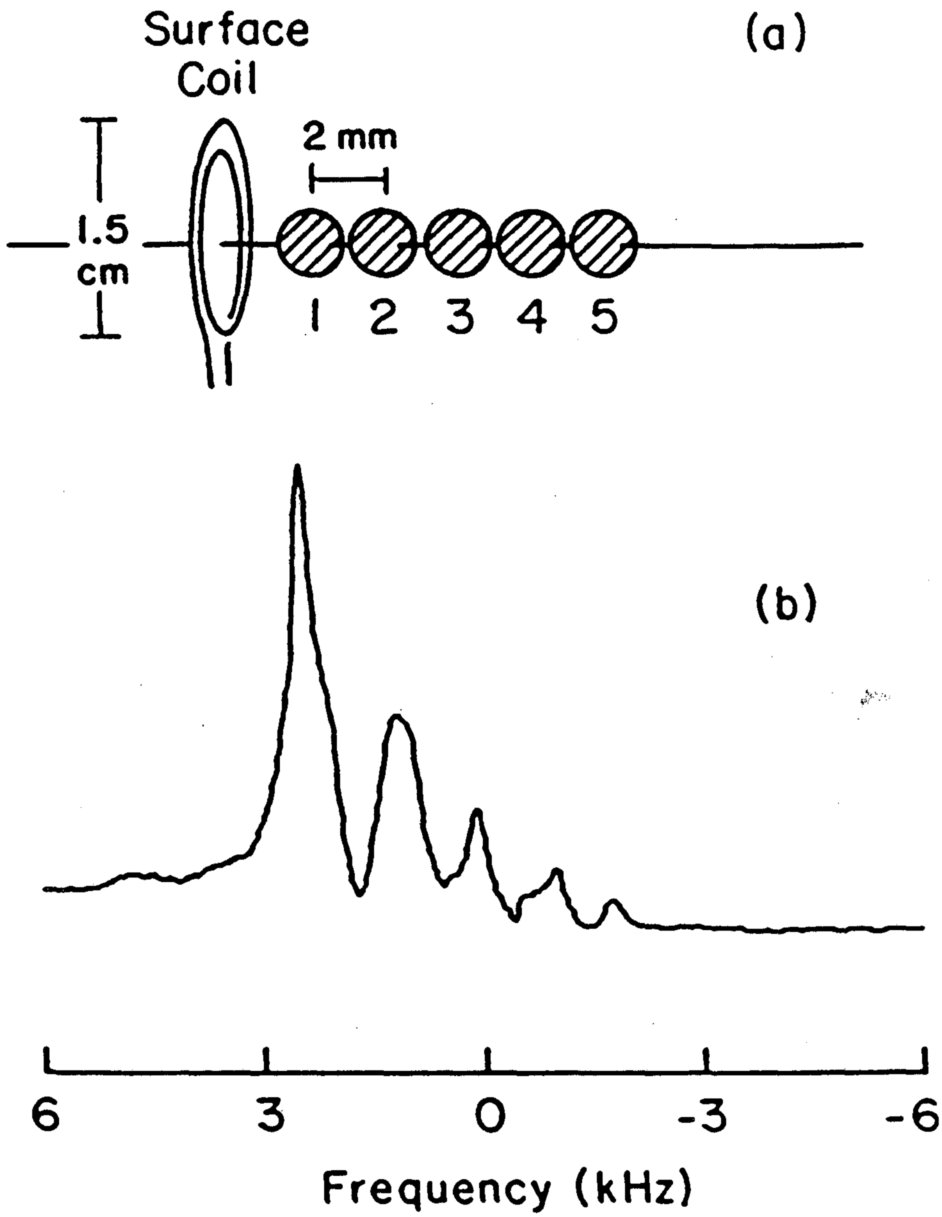

Figure 3

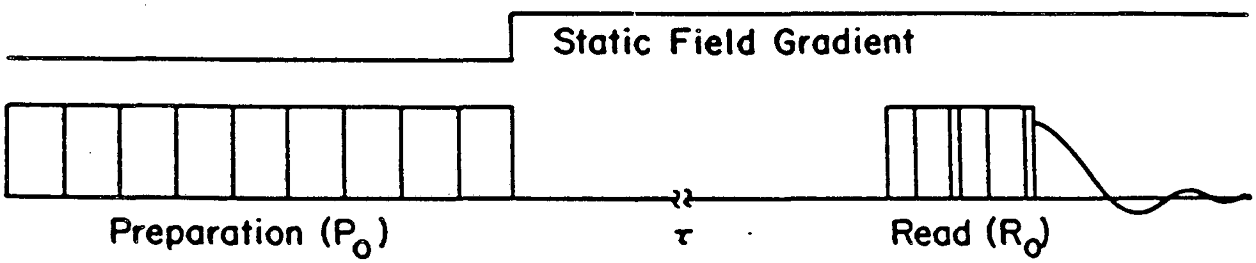

Figure 4

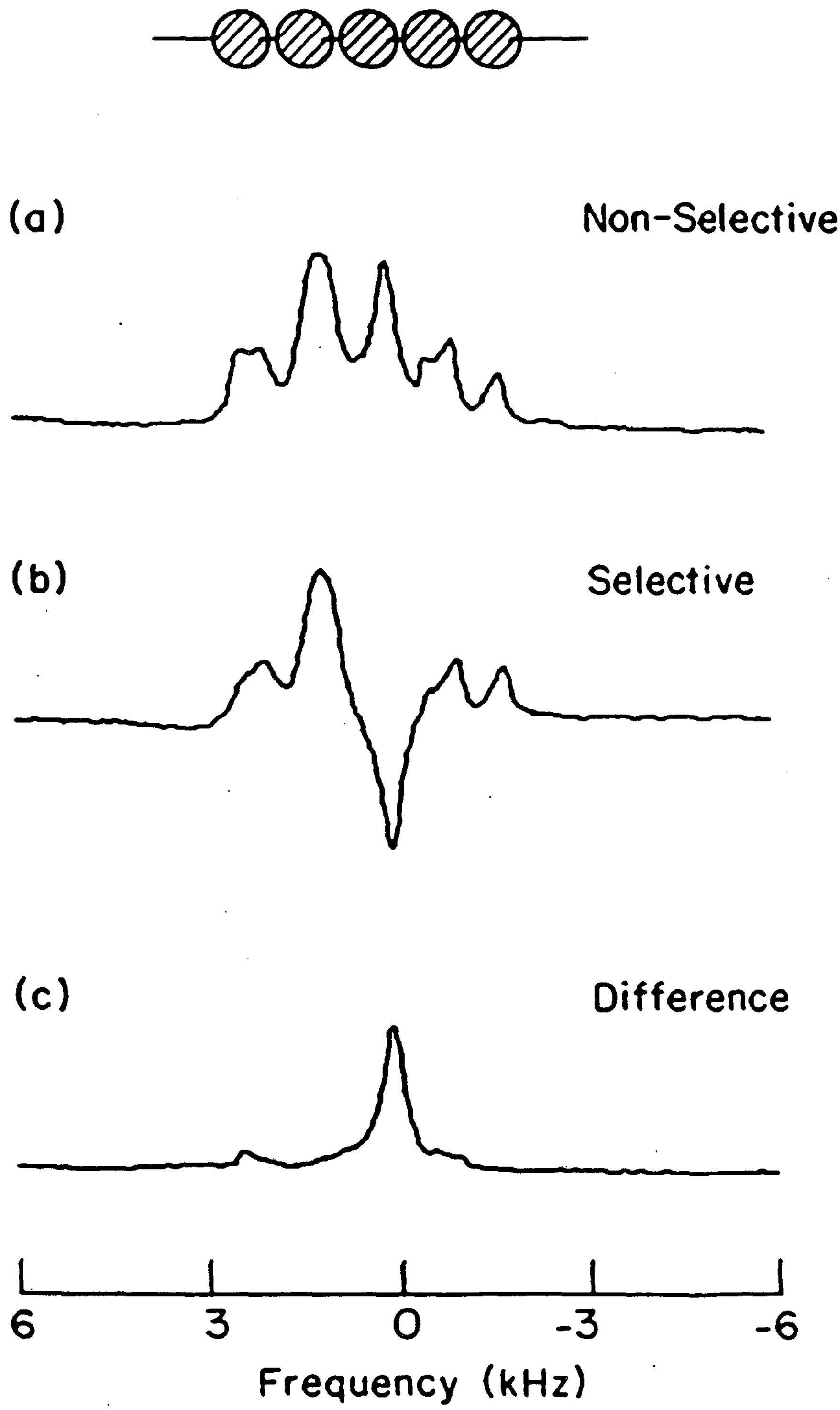
(a)
Non-Selective
(b)
Selective
(c)
Difference
6
3
0
-3
-6
Frequency (kHz)

Figure 5

Figure 6

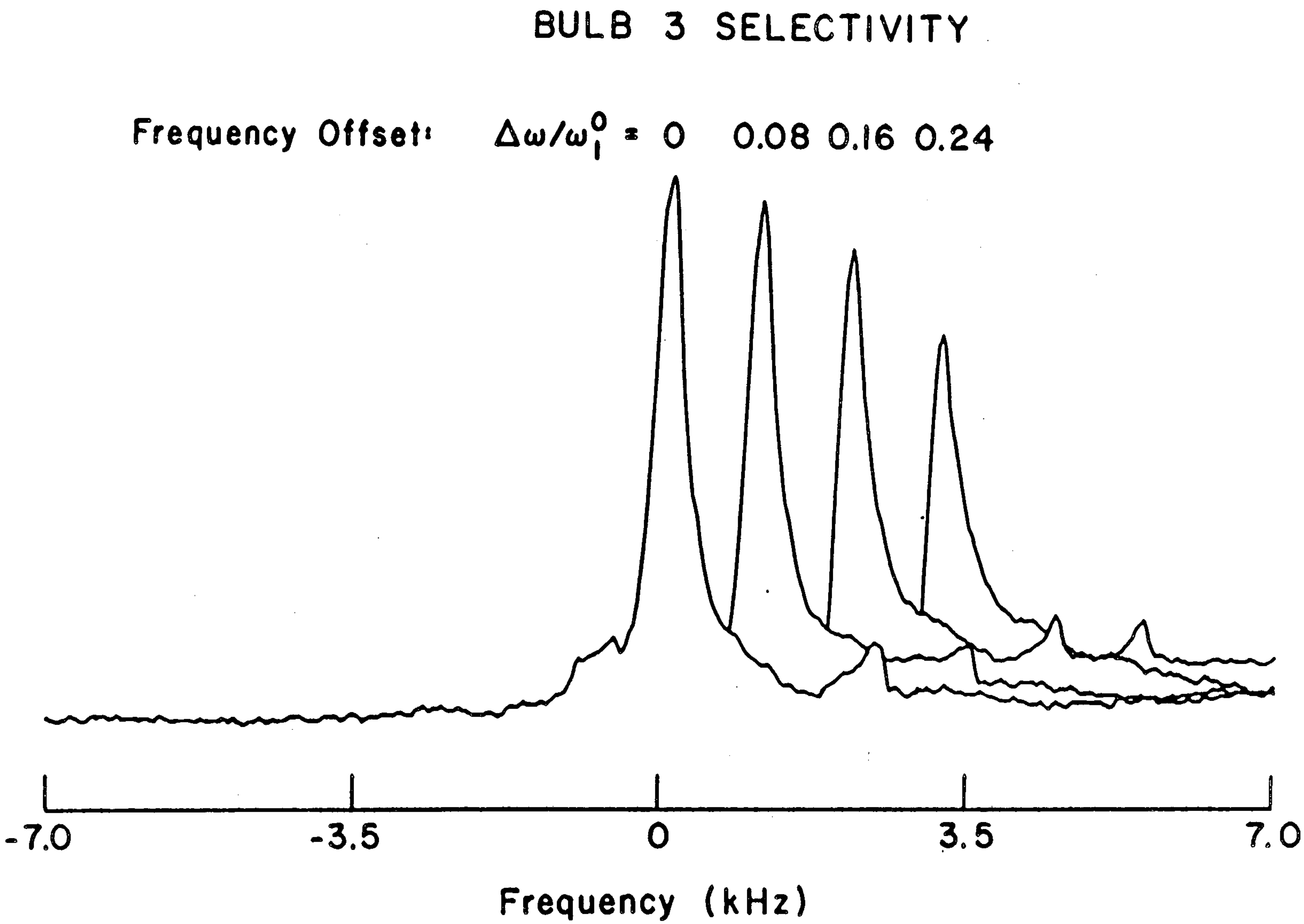

BULB 3 SELECTIVITY
Frequency Offset: $\Delta\omega/\omega_1^0$ = 0 0.08 0.16 0.24
-7.0
-3.5
0
3.5
7.0
Frequency (kHz)